CHIN. PHYS. LETT. Vol. 38, No. 1 (2021) 018101

Prediction of Superhard BN_2 with High Energy Density

Yiming Zhang(张逸铭)[1†], Shuyi Lin(林舒怡)[1†], Min Zou(邹敏)[1], Meixu Liu(刘玫序)[1], Meiling Xu(徐美玲)[1*], Pengfei Shen(申鹏飞)[2], Jian Hao(郝健)[1*], and Yinwei Li(李印威)[1]

[1]*Laboratory of Quantum Functional Materials Design and Application, School of Physics and Electronic Engineering, Jiangsu Normal University, Xuzhou 221116, China*

[2]*Academy for Advanced Interdisciplinary Studies, Southern University of Science and Technology, Shenzhen 518055, China*

(Received 7 October 2020; accepted 9 November 2020; published online 6 January 2021)

Considering that pressure-induced formation of short, strong covalent bonds in light-element compounds can produce superhard materials, we employ structure searching and first-principles calculations to predict a new class of boron nitrides with a stoichiometry of BN_2, which are stable relative to alpha-B and alpha-N_2 at ambient pressure. At ambient pressure, the most stable phase has a layered structure (h-BN_2) containing hexagonal BN layers between which there are intercalated N_2 molecules. At 25 GPa, a three-dimensional $P4_2/mmc$ structure with single N–N bonds becomes the most stable. Dynamical, thermal, and mechanical stability calculations reveal that this structure can be recovered under ambient conditions. Its calculated stress-strain relations demonstrate an intrinsic superhard nature with an estimated Vickers hardness of ∼43 GPa. This structure has a potentially high energy density of ∼4.19 kJ/g.

DOI: 10.1088/0256-307X/38/1/018101

Diamond is a typical superhard material, however there exist various limitations to hinder its widespread applications. It is brittle, easily oxidizes to carbon dioxide at high temperature in air, and can react with Fe-containing materials.[1,2] Isostructural to diamond, *c*-BN is chemically stable and also superhard, but the synthesis of large crystals has been a great challenge.[3,4] Therefore, the search for novel superhard materials with excellent mechanical properties that are more stable than diamond or *c*-BN has been a long-standing goal in physics and materials science.

Two types of materials are of special interest.[5–32] One concerns compounds of transition metals and light elements that have high valence electron density and strongly directional covalent bonds, including OsN_2, IrN_2, W–N compounds, TiB_2, ZrB_6, and WB_4. The presence of metallic bonds and lack of orientation of ionic bonds reduce the hardness of these materials (<40 GPa). The other type includes light-element compounds composed of B, C, N, and O with short and strong covalent bonds, such as diamond-like BC_3, BC_5, BC_2N, BC_4N, C_3N_4, *o*-C_3N, B_4CO_4, B_2CO, and BC_8N. The synthesis of these materials and determination of their atomic site occupation continue to face challenges owing to being stabilized in narrow ranges of pressure and temperature, and the similar atomic sizes of their constituents.

Boron and nitride can easily form strong covalent bonds at high pressure, and much research effort has explored superhard boron nitride materials such as *c*-BN,[3,4] *w*-BN,[33] *p*-BN,[34] *bct*-BN,[35] *o*-BN,[35,36] M-BN,[37] $Pmn2_1$ BN,[38] *t*-BN,[39] *cm*-BN,[40] Z-BN,[41] *Pbca*-BN,[42] and *pct*-BN,[43] which possess estimated Vickers hardness values of 47–67 GPa. Recently reported non-stoichiometric B–N compounds, such as B_6N,[44,45] B_3N_5,[46] B_3N_4,[47] B_2N_3,[48] $B_{13}N_2$,[49–53] are potential new superhard materials. In contrast to insulating BN, some of these compounds[46–48] are narrow-band-gap semiconductors or even conductors, making them potentially useful in electronic devices at high pressure.

High pressure can efficiently break the strong intramolecular triple N≡N bonds for the formation of single N–N bonds.[54,55] The remarkable difference in the average bond energy between single N–N bonds and triple N≡N bonds makes most high-pressure B–N compounds high-energy density materials. This work reports first-principles calculations that predict the structures of BN_2. A $P4_2/mmc$-BN_2 structure emerged as a superhard material with a Vickers hardness of ∼43 GPa. It has a high energy density of ∼4.19 kJ/g.

Computational Methods. The structure of BN_2 (1–4 formula units) was predicted at pressures of 0–

Supported by the National Natural Science Foundation of China (Grant Nos. 12074154, 11904142 and 11722433), the Science and Technology Project of Xuzhou (Grant No. KC19010), the Six Talent Peaks Project and the 333 High-Level Talents Project of Jiangsu Province, and the Natural Science Research Projects of Colleges and Universities in Jiangsu Province (Grant No. 19KJB140001).

*Corresponding author. Email: xml@calypso.cn; jian_hao@jsnu.edu.cn

†Yiming Zhang and Shuyi Lin contributed equally to this work.

50 GPa using particle swarm optimization as implemented in CALYPSO code.[56–61] Structure optimization and electronic properties were calculated using density functional theory within the generalized gradient approximation expressed by the Perdew–Burke–Ernzerhof functional,[62] as implemented in the Vienna *ab initio* simulation package.[63] The projector augmented wave method[64] was adopted for B and N atoms with valence electrons of $2s^22p^1$ and $2s^22p^3$, respectively. A kinetic cutoff energy of 520 eV and Monkhorst–Pack k meshes with a grid spacing of $2\pi \times 0.03\,\text{Å}^{-1}$ were adopted to obtain converged total energies (∼1 meV per atom) and converged forces (0.01 eV·Å^{-1} per atom). The dynamic stability of the predicted structures with $3\times3\times2$ supercells was identified from phonon calculation using the direct supercell method as implemented in PHONOPY code.[65,66] Thermal stability was confirmed by *ab initio* molecular dynamics simulations carried out with a time step of 1 fs and a total simulation time of 7 ps. The temperature was maintained at 300 K using a Nosé Hoover chain thermostat with $3\times3\times2$ supercells. Bulk, shear, and Young's moduli were estimated in the Voigt–Reuss–Hill approximation.[67] The ideal tensile and shear strengths in various lattice directions were estimated by calculating stress–strain relations using an established method.[29,68,69] As standard generalized gradient approximation tends to underestimate band gaps, we also employed the Heyd–Scuseria–Ernzerhof (HSE) hybrid functional,[70] which can reliably calculate electronic structures, to evaluate band gaps.

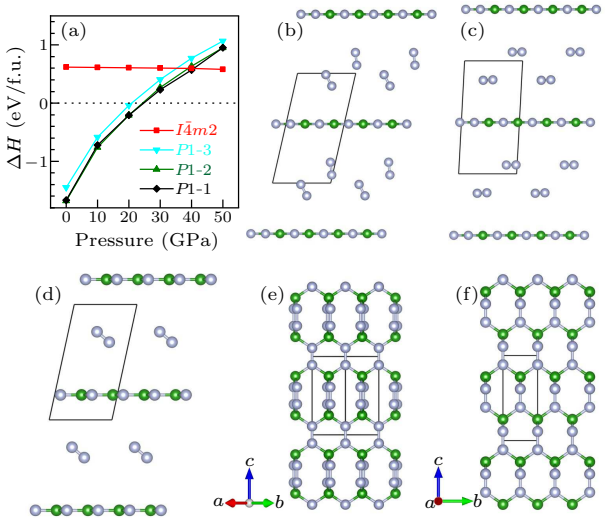

Fig. 1. (a) Enthalpy versus pressure for various BN_2 structures relative to that of the $P4_2/mmc$ phase. Crystal structures of (b)–(d) $P1$, (e) $P4_2/mmc$, and (f) $I\bar{4}m2$. Light grey and green spheres represent N and B atoms, respectively. The f.u. stands for formula unit.

Results and Discussion. The structure search results in Fig. 1(a) show three low-energy layered structures for BN_2 (h-BN_2) with space group $P1$ at ambient pressure. Similar to the layered structures predicted for various B–N compounds, such as B_2N_3[48] and B_3N_5,[46] h-BN_2 has the same hexagonal BN layers, between which there are interstitial N_2 molecules [Figs. 1(b)–1(d)]. The N_2 molecules are oriented differently in the three energetically comparable layered structures, indicating relatively weak interaction between them and the BN layers. The B–N bond length in each BN layer is 1.45 Å, as the same as in h-BN.[71] The N≡N triple bonds (1.11 Å) are slightly longer than those (1.07 Å) in pure N_2.[72] This work is aimed at searching for superhard materials with high energy density. The layered structures at ambient pressure do not meet the requirements owing to weak van der Waals interaction between the layers and to the existence of triple N≡N bonds, thus we do not focus on the layered structures.

At 25 GPa, h-BN_2 transforms to a tetragonal three-dimensional structure with space group $P4_2/mmc$. Although this structure is also predicted at ambient pressure, it has a greater enthalpy than h-BN_2. As illustrated in Fig. 1(e), the triple N≡N bonds of the interstitial N_2 transform to the single N–N bonds at high pressure, and the nitrogen atoms also bond with the neighboring BN layers, linking them in a BNNB stacking sequence. At ambient pressure, the B–N bond length is calculated to be 1.56 Å in $P4_2/mmc$ BN_2, which is slightly longer than that in h-BN. The structure's N–N single bond length is 1.33 Å. Structure searching also finds a metastable BN_2 phase, akin to $P4_2/mmc$ BN_2, which consists of BN blocks connected by single N–N bonds [space group $I\bar{4}m2$, Fig. 1(f)]. Table 1 lists the information about both structures.

Table 1. Lattice parameters of the $P4_2/mmc$ and $I\bar{4}m2$ structures at ambient pressure.

Space group	Lattice parameter (Å)	Atomic position
$P4_2/mmc$	$a = b = 3.655$	B1($4d$) (0.5, 0, 0.25)
	$c = 6.093$	N1($8j$) (0.773, 0.227, 0.391)
$I\bar{4}m2$	$a = b = 2.541$	B1($2d$) (0, 0.5, 0.75)
	$c = 6.224$	N1($4e$) (0, 0, 0.892)

The formation energies of BN systems (such as h-BN and B_6N) relative to alpha-B and alpha-N_2 have been calculated at ambient pressure. Although BN_2 is unstable and will decompose into h-BN and N_2, it has a negative formation energy (−0.29 eV/atom) respective to alpha-B and alpha-N_2, implying the possibility of synthesis using alpha-B and alpha-N_2 as precursors. Additionally, BN_2 is also stable with respective to B_6N which has been synthesized in experiment and alpha-N_2. The calculated phonon dispersions show an absence of any imaginary frequencies in the whole Brillouin zone, confirming that the $P4_2/mmc$ and $I\bar{4}m2$ structures are dynamically stable both at 0 and 30 GPa [Figs. 2(a) and 2(b)]. The ther-

mal stability of these structures is explored through molecular dynamics simulations. Heating to 300 K for 7 ps revealed no structure distortions, indicating that the structures are metastable under ambient conditions [Figs. 2(c) and 2(d)].

The calculated elastic constants of both the structures identify their mechanical stability (Table 2). The set of elastic constants must satisfy the following mechanical stability criteria for a tetrahedral crystal: $C_{ii} > 0$ $(i = 1, 3, 4, 6)$, $(C_{11} - C_{12}) > 0$, $(C_{11} + C_{33} - 2C_{13}) > 0$, and $[2(C_{11} + C_{12}) + C_{33} + 4C_{13}] > 0$. The calculated results verify the mechanical stability of both the structures. Their C_{33} values are both greater than those of diamond[69] or *c*-BN,[46] indicating high incompressibility along the *c*-axis. The independent elastic constants can be used to derive the bulk (B_0) and shear (G_0) moduli, whose values are 338 and 274 GPa, respectively, for the $P4_2/mmc$ phase and slightly lower (299 and 218 GPa, respectively) for the $I\bar{4}m2$ phase. Although these values are less than those of diamond, they are comparable to those of B–N superhard compounds, owing to the similar bond configurations: for example, $C222_1$-B_3N_5 (B_0, 328 GPa; G_0, 289 GPa)[46] and *t*-B_2N_3 (B_0, 337 GPa; G_0, 300 GPa).[48] Furthermore, the G_0/B_0 ratio of the $P4_2/mmc$ phase (0.86) is close to those (0.9–1.2) of typical superhard materials,[73] indicating that it is a potential superhard material. In contrast, the G_0/B_0 ratio of $I\bar{4}m2$ phase is only 0.73, which suggests that it is hard rather than superhard. The Pugh ratio (B_0/G_0) is defined as a quantitative index for assessing the brittle or ductile behavior of crystals. According to Pugh, B_0/G_0 values of >1.75 and <1.75 represent ductile and brittle, respectively. The Pugh values of $P4_2/mmc$ and $I\bar{4}m2$ phases are calculated to be 1.23 and 1.37, respectively, demonstrating they are brittle.

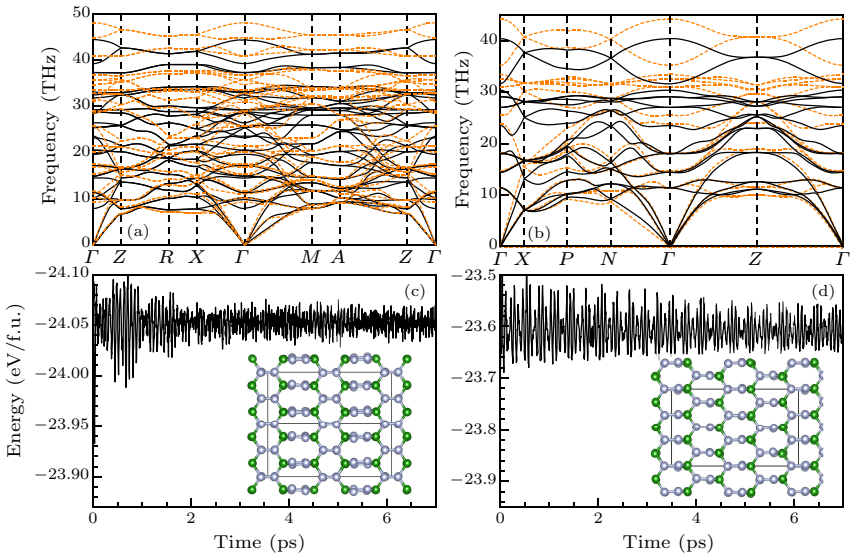

Fig. 2. Phonon dispersion curves of (a) $P4_2/mmc$ BN_2 and (b) $I\bar{4}m2$ BN_2 at both 0 GPa (black solid lines) and 30 GPa (orange dotted lines). Energy fluctuations during molecular dynamics simulations up to 7 ps for (c) $P4_2/mmc$ and (d) $I\bar{4}m2$-BN_2 at 0 GPa and 300 K.

Table 2. Calculated elastic constants C_{ij} (GPa), bulk modulus B_0 (GPa), shear modulus G_0 (GPa), G_0/B_0, Young's modulus E_0 (GPa), and Poisson's ratio (P_r) of $P4_2/mmc$ BN_2, $I\bar{4}m2$ BN_2, diamond, and *c*-BN.

Phases	C_{11}	C_{22}	C_{33}	C_{44}	C_{55}	C_{66}	C_{12}	C_{13}	C_{23}	B_0	G_0	G_0/B_0	E_0	P_r
$P4_2/mmc$	421		1077	285		319	235	118		338	274	0.86	639	0.16
$I\bar{4}m2$	552		1143	274		76	58	129		299	218	0.72	526	0.21
Diamond	1050			561			124			434	564	1.3	1181	0.05
c-BN	779			443			190			373	388	1.04	913	0.12

Stress–strain relations for the $P4_2/mmc$ phase calculated along different directions provide some insight into the mechanisms of local bond deformation and breaking, which underlie the intrinsic mechanical properties of a material. Tensile stresses along high-symmetry directions are first examined to find the weakest tensile directions that determine easy cleavage planes. The results in Fig. 3(a) show that the $P4_2/mmc$ phase has strong stress responses in the ⟨100⟩ and ⟨001⟩ directions, with a peak tensile stress between 110 and 165 GPa. The ⟨111⟩ direction is the weakest tensile direction; its ideal strength of 48 GPa is comparable to that of *o*-CN (41 GPa) and C_3N_4 (45 GPa).[69]

We next evaluate the shear stress response in the (111) easy cleavage planes of the $P4_2/mmc$ phase. An ideal shear strength of 43 GPa is obtained in the (111)[30$\bar{2}$] direction [Fig. 3(b)]; though lower than that of diamond, it is still higher than the typical threshold for superhard materials (40 GPa), and is comparable to that of t-B_3N_4 (42.5 GPa)[47] and $C222_1$ B_3N_5 (44 GPa),[46] confirming the superhard nature of the $P4_2/mmc$ phase.

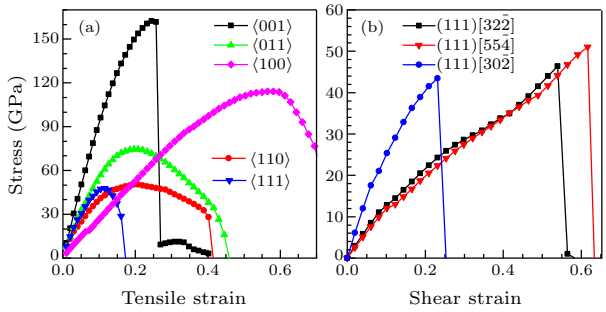

Fig. 3. (a) Calculated tensile stress–strain relations for $P4_2/mmc$ BN_2 in various directions. (b) Calculated shear stress–strain relations for the (111) easy cleavage planes of $P4_2/mmc$ BN_2.

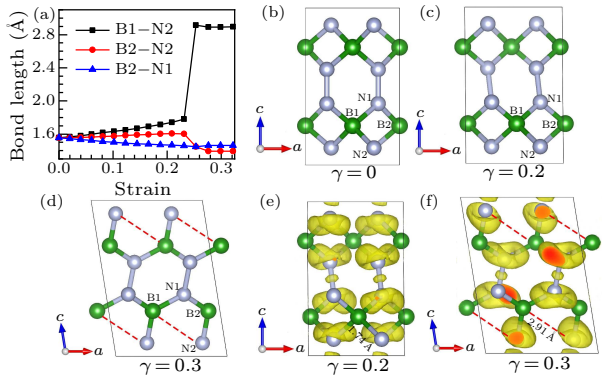

Fig. 4. (a) Bond lengths under (111)[30$\bar{2}$] shear strain, and (b)–(d) related structural snapshots with 3D electron localization functions (isovalue = 0.8) at shear strains of (e) 0.2 and (f) 0.3.

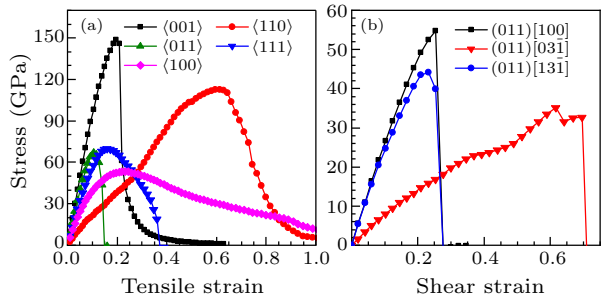

Fig. 5. (a) Calculated tensile stress–strain relations for $I\bar{4}m2$ BN_2 in various directions. (b) Calculated shear stress–strain relations for the (011) easy cleavage planes of $I\bar{4}m2$ BN_2.

The mechanisms of local bond deformation and breaking are explored by considering the evolution of bond lengths in the $P4_2/mmc$ phase under (111)[30$\bar{2}$] shear strain. The plots in Fig. 4(a) show a sharp increase in B1–N2 bond length at a strain of 0.23, corresponding to the peak shear stress. The B2–N2 bond length suddenly decreases simultaneously, because each N2 atom connects with both B1 and B2 atoms, and the N2 atoms will inevitably be closer to the B2 atoms once the B1–N2 bonds break. Structural snapshots and the corresponding electron localization function before and after the shear instability under (111)[30$\bar{2}$] shear strain are exhibited in Figs. 4(b)–4(f). The B1–N2 bonds clearly break after the strain reaches 0.23 given the absence of any electron localization, indicating that the B1–N2 bonds are the main load-bearing component.

To quantify the hardness of $I\bar{4}m2$ phase, we also calculated the stress–strain relations. As seen from Fig. 5(a), the ⟨011⟩ direction is the weakest tensile direction and its ideal strength is 66 GPa. We next evaluate the shear stress response in the (011) easy cleavage plane, and its ideal shear strength of 35 GPa is obtained in the (011)[03$\bar{2}$] direction. Therefore, the estimated Vickers hardness of $I\bar{4}m2$ phase is 35 GPa, suggesting that it is hard rather than superhard.

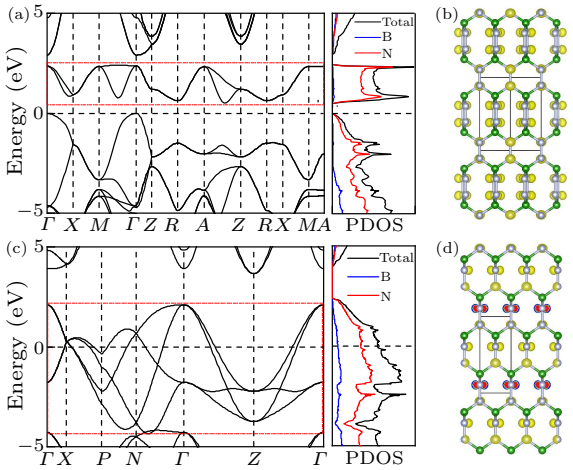

Fig. 6. Band structures and PDOS [in units of states/(eV·f.u.)] of (a) $P4_2/mmc$ BN_2 and (c) $I\bar{4}m2$ BN_2 at 0 GPa at the HSE06 level. The band decomposed charge density of (b) $P4_2/mmc$ BN_2 and (d) $I\bar{4}m2$ BN_2 (marked by the red dashed rectangular frame).

The calculated band structures and projected density of states (PDOS) of the $P4_2/mmc$ and $I\bar{4}m2$ structures in Fig. 6 show that, in contrast to the large band gaps of h-BN_2 and the various crystalline forms of BN, $P4_2/mmc$ BN_2 is a semiconductor with a small band gap of 0.5 eV at the HSE06 level, and $I\bar{4}m2$ BN_2 exhibits metallic properties. We have calculated the band decomposed charge density to confirm the conductive direction in $I\bar{4}m2$ BN_2. The calculated charge density of $I\bar{4}m2$ phase is from four bands across the Fermi level (highlight in the red dashed rectangular frame). As seen from Fig. 6, the charge density across the Fermi level of $I\bar{4}m2$ phase is entirely con-

tributed by the π orbitals of N–N band spreading in a–b planes, indicating that it is two-dimensionally conductive. A small metallic component generally lessens the hardness of covalent crystals strongly, due to electron delocalization,[74] and the present hardness calculations follow this trend. We calculated the energy involved in the BN_2 decomposed into h-BN and alpha-N_2 at ambient pressure. The reason we choose h-BN and alpha-N_2 as decomposition product is that they are stable at ambient pressure and have been synthesized in experiment. The energy difference is calculated to be 1.69 eV, which corresponds to an energy density of 4.19 kJ/g, indicating that $P4_2/mmc$ BN_2 is a promising high-energy-density material.

In summary, we have calculated crystal structures of BN_2 at 0–50 GPa using CALYPSO code. A tetragonal three-dimensional $P4_2/mmc$-BN_2 structure containing single N–N bonds is predicted to be energetically most stable above 25 GPa. Furthermore, it could be recovered under ambient conditions. Its calculated electronic band structure shows that it is a semiconductor with a narrow band gap of 0.5 eV. Significantly, $P4_2/mmc$ BN_2 is a multi-role material combining superhardness (Vickers hardness of ∼43 GPa) and high-energy density (∼4.19 kJ/g).

The calculations were performed in the School of Physics and Electronic Engineering of Jiangsu Normal University.

References

[1] Kumaran C R, Tiwari B, Chandran M, Bhattacharya S S and Ramachandra R M S 2013 *J. Nanopart. Res.* **15** 1509
[2] Meng D, Yue W, Lin F, Wang C and Wu Z 2015 *J. Superhard Mater.* **37** 67
[3] Dong G Y, Yang X D, Li X B, Song X S and Cheng X L 2008 *Diamond Relat. Mater.* **17** 1
[4] Zhang Y, Sun H and Chen C 2006 *Phys. Rev. B* **73** 144115
[5] Liu H, Fan Q Y, Yang F, Yu X H, Zhang W and Yun S N 2020 *Chin. Phys. B* **29** 106102
[6] Young A F, Sanloup C, Gregoryanz E, Scandolo S, Hemley R J and Mao H 2006 *Phys. Rev. Lett.* **96** 155501
[7] Xu X, Chai C, Fan Q and Yang Y 2017 *Chin. Phys. B* **26** 046101
[8] Ma Z, Wang P, Yan F, Shi C and Tian Y 2019 *Chin. Phys. B* **28** 036101
[9] Crowhurst J C 2006 *Science* **311** 1275
[10] Wang S, Yu X, Lin Z, Zhang R, He D, Qin J, Zhu J, Han J, Wang L, Mao H, Zhang J and Zhao Y 2012 *Chem. Mater.* **24** 3023
[11] Lu C, Li Q, Ma Y and Chen C 2017 *Phys. Rev. Lett.* **119** 115503
[12] Solozhenko V L, Andrault D, Fiquet G, Mezouar M and Rubie D C 2001 *Appl. Phys. Lett.* **78** 1385
[13] Luo X, Zhou X F, Liu Z, He J, Xu B, Yu D, Wang H T and Tian Y 2008 *J. Phys. Chem. C* **112** 9516
[14] Qu N R, Wang H C, Li Q, Li Y D, Li Z P, Gou H Y and Gao F M 2019 *Chin. Phys. B* **28** 096201
[15] Wang S, Oganov A R, Qian G, Zhu Q, Dong H, Dong X and Davari E M M 2016 *Phys. Chem. Chem. Phys.* **18** 1859
[16] Pan Y, Xie C, Xiong M, Ma M, Liu L, Li Z, Zhang S, Gao G, Zhao Z, Tian Y, Xu B and He J 2017 *Chem. Phys. Lett.* **689** 68
[17] Bundy F P and Kasper J S 1967 *J. Chem. Phys.* **46** 3437
[18] Guo W F, Wang L S, Li Z P, Xia M R and Gao F M 2015 *Chin. Phys. Lett.* **32** 096201
[19] Knotek O, Breidenbach R, Jungblut F and Löffler F 1990 *Surf. Coat. Technol.* **43–44** 107
[20] Wang D, Shi R and Gan L H 2017 *Chem. Phys. Lett.* **669** 80
[21] Li X and Peng F 2019 *Phys. Chem. Chem. Phys.* **21** 15609
[22] Gu Q, Krauss G and Steurer W 2008 *Adv. Mater.* **20** 3620
[23] Zinin P V, Ming L C, Ishii H A, Jia R, Acosta T and Hellebrand E 2012 *J. Appl. Phys.* **111** 114905
[24] Solozhenko V L, Kurakevych O O, Andrault D, Le G Y and Mezouar M 2009 *Phys. Rev. Lett.* **102** 015506
[25] Hu Y J, Xu S L, Wang H, Liu H, Xu X C and Cai Y X 2016 *Chin. Phys. Lett.* **33** 106102
[26] Li Q, Wang M, Oganov A R, Cui T, Ma Y and Zou G 2009 *J. Appl. Phys.* **105** 53514
[27] Qu N R, Wang H C, Li Q, Li Z P and Gao F M 2019 *Chin. Phys. Lett.* **36** 036201
[28] Horvath-Bordon E, Riedel R, Zerr A, McMillan P F, Auffermann G, Prots Y, Bronger W, Kniep R and Kroll P 2006 *Chem. Soc. Rev.* **35** 987
[29] Hao J, Liu H, Lei W, Tang X, Lu J, Liu D and Li Y 2015 *J. Phys. Chem. C* **119** 28614
[30] Ma Z Y, Yan F, Wang S X, Jia Q Q, Yu X H and Shi C L 2017 *Chin. Phys. B* **26** 126105
[31] Li Y, Li Q and Ma Y 2011 *Europhys. Lett.* **95** 66006
[32] Gao Y, Ying P, Wu Y, Chen S, Ma M, Wang L, Zhao Z and Yu D 2019 *J. Appl. Phys.* **125** 175108
[33] Xu N, Li J F, Huang B L and Wang B L 2016 *Chin. Phys. B* **25** 016103
[34] Long J, Shu C, Yang L and Yang M 2015 *J. Alloys Compd.* **644** 638
[35] Zhang Z, Lu M, Zhu L, Zhu L, Li Y, Zhang M and Li Q 2014 *Phys. Lett. A* **378** 741
[36] Huang Q, Yu D, Zhao Z, Fu S, Xiong M, Wang Q, Gao Y, Luo K, He J and Tian Y 2012 *J. Appl. Phys.* **112** 53518
[37] Zhang X, Wang Y, Lv J, Zhu C, Li Q, Zhang M, Li Q and Ma Y 2013 *J. Chem. Phys.* **138** 114101
[38] Jiang X, Zhao J and Ahuja R 2013 *J. Phys.: Condens. Matter* **25** 122204
[39] Li S, Shi L, Zhu H, Xia W and Wang Y 2019 *Phys. Status Solidi* **256** 1800699
[40] Tian Y, Kou C, Lu M, Yan Y, Zhang D, Li W, Cui X, Zhang S, Zhang M and Gao L 2020 *Phys. Lett. A* **384** 126518
[41] He C, Sun L, Zhang C, Peng X, Zhang K and Zhong J 2012 *Phys. Chem. Chem. Phys.* **14** 10967
[42] Fan Q, Wei Q, Yan H, Zhang M, Zhang Z, Zhang J and Zhang D 2014 *Comput. Mater. Sci.* **85** 80
[43] Li Z and Gao F 2012 *Phys. Chem. Chem. Phys.* **14** 869
[44] Hubert H, Garvie L A J, Buseck P R, Petuskey W T and Mcmillan P F 1997 *J. Solid State Chem.* **133** 356 10.1006/jssc.1997.7582
[45] Solozhenko V L, Le G Y and Kurakevych O O 2006 *C. R. Chim.* **9** 1472
[46] Li Y, Hao J, Liu H, Lu S and Tse J S 2015 *Phys. Rev. Lett.* **115** 105502
[47] Xie C, Ma M, Liu C, Pan Y, Xiong M, He J, Gao G, Yu D, Xu B, Tian Y and Zhao Z 2017 *J. Mater. Chem. C* **5** 5897
[48] Lin S, Xu M, Hao J, Wang X, Wu M, Shi J, Cui W, Liu D, Lei W and Li Y 2019 *J. Mater. Chem. C* **7** 4527
[49] Solozhenko V L and Kurakevych O O 2008 *J. Phys.: Conf. Ser.* **121** 62001
[50] Zhang H, Yao S and Widom M 2016 *Phys. Rev. B* **93** 144107
[51] Ektarawong A, Simak S I and Alling B 2017 *Phys. Rev. B* **95** 064206
[52] Kurakevych O O and Solozhenko V L 2007 *Acta Crystallogr. Sect. C: Cryst. Struct. Commun.* **63** i80
[53] Solozhenko V L and Turkevich V Z 2018 *J. Phys. Chem. C*

122 8505
[54] Steele B A and Oleynik I I 2016 *Chem. Phys. Lett.* **643** 21
[55] Shi X H, Liu B, Yao Z and Liu B B 2020 *Chin. Phys. Lett.* **37** 047101
[56] Gao B, Gao P, Lu S, Lv J, Wang Y and Ma Y 2019 *Sci. Bull.* **64** 301
[57] Wang Y, Lv J, Zhu L and Ma Y 2010 *Phys. Rev. B* **82** 094116
[58] Wang Y, Lv J, Zhu L and Ma Y 2012 *Comput. Phys. Commun.* **183** 2063
[59] Cui W and Li Y 2019 *Chin. Phys. B* **28** 107104
[60] Li L, Cui X, Cao H, Jiang Y, Duan H, Jing Q, Liu J and Wang Q 2020 *Chin. Phys. B* **29** 077101
[61] Sun Y, Xu B and Yi L 2020 *Chin. Phys. B* **29** 023102
[62] Perdew J P, Burke K and Ernzerhof M 1996 *Phys. Rev. Lett.* **77** 3865
[63] Kresse G and Furthmüller J 1996 *Phys. Rev. B* **54** 11169
[64] Kresse G and Joubert D 1999 *Phys. Rev. B* **59** 1758
[65] Togo A, Oba F and Tanaka I 2008 *Phys. Rev. B* **78** 134106
[66] Parlinski K, Li Z Q and Kawazoe Y 1997 *Phys. Rev. Lett.* **78** 4063
[67] Hill R 1952 *Proc. Phys. Soc. A* **65** 349
[68] Roundy D, Krenn C R, Cohen M L and Morris J W 1999 *Phys. Rev. Lett.* **82** 2713
[69] Tang X, Hao J and Li Y 2015 *Phys. Chem. Chem. Phys.* **17** 27821
[70] Heyd J, Scuseria G E and Ernzerhof M 2003 *J. Chem. Phys.* **118** 8207
[71] Paine R T and Narula C K 1990 *Chem. Rev.* **90** 73
[72] Gall D, Shin C S, Spila T, Odén M, Senna M J H, Greene J E and Petrov I 2002 *J. Appl. Phys.* **91** 3589
[73] Wu Z, Zhao E, Xiang H, Hao X, Liu X and Meng J 2007 *Phys. Rev. B* **76** 054115
[74] Guo X, Li L, Liu Z, Yu D, He J, Liu R, Xu B, Tian Y and Wang H T 2008 *J. Appl. Phys.* **104** 23503